

# Modulation of the Curie Temperature in Ferromagnetic/Ferroelectric Hybrid Double Quantum Wells

N. Kim<sup>1</sup>, H. Kim<sup>2</sup>, J. W. Kim<sup>1</sup>, S. J. Lee<sup>1</sup>, and T. W. Kang<sup>1</sup>

<sup>1</sup>Quantum-functional Semiconductor Research Center,

Dongguk University, Seoul 100-715, Korea

<sup>2</sup>Department of Physics, Soongsil University, Seoul 156-743, Korea

(Dated: December 9, 2005)

## Abstract

We propose a ferromagnetic/ferroelectric hybrid double quantum well structure, and present an investigation of the Curie temperature ( $T_C$ ) modulation in this quantum structure. The combined effects of applied electric fields and spontaneous electric polarization are considered for a system that consists of a Mn-doped well, a barrier, and a p-type ferroelectric well. We calculate the change in the envelope functions of carriers at the lowest energy subband, resulting from applied electric fields and switching the dipole polarization. By reversing the depolarizing field, we can achieve two different ferromagnetic transition temperatures of the ferromagnetic quantum well in a fixed applied electric field. The Curie temperature strongly depends on the position of the Mn-doped layer and the polarization strength of the ferroelectric well.

---

Electronic mail: nmikim@dongguk.edu

The diluted magnetic semiconductor (DMS) has been generally known as one of the promising candidates for spintronic device materials in virtue of the coexistence of ferromagnetic and semiconducting properties in it. Ferroelectric material has also attracted significant interest because of its promising potential in various technological applications, such as binary data storage media in nonvolatile random access memories due to its spontaneous electric polarization. In both research fields, many experimental and theoretical studies have been performed.

Because the spintronic devices should ultimately be operated at room temperature, much effort has been focused on increasing the ferromagnetic transition temperature ( $T_c$ ) of DMS above room temperature. Among many materials, ZnMnO is considered to have  $T_c$  above 300 K with 5% Mn per unit cell and  $3 \times 10^{20}$  holes per  $\text{cm}^3$  according to a theoretical prediction.[1]

Recently, observation of the ferroelectric properties was reported in Li-doped ZnO bulk samples.[2, 3] The reason for the ferroelectric property is attributed to the following: when the size of the dopant Li atom (0.6 Å) is smaller than the host Zn atom (0.74 Å) [2], then the Li atoms can occupy off-center positions, thus locally inducing electric dipoles, thereby leading to ferroelectric behavior like PbGeTe[4] ferroelectric semiconductor (FES).

The mechanism of DMS ferromagnetism is classified upon materials and growing techniques. The first class of approach is ferromagnetism due to the Ruderman-Kittel-Kasuya-Yoshida (RKKY)/Zener indirect exchange interaction by delocalized holes (hole mediated) based on the mean-field approximation.[5, 6] The second class of approach is also carrier-induced ferromagnetism as a results of KKR-CPA-LDA (Korringa-Kohn-Rostoker coherent-potential approximation and local density approximation) calculations of the electronic structure of doped DMS alloys.[7, 8] The third class of approach suggests the hole hopping mediated ferromagnetism between polarons having strongly localized charge carriers.[9, 10] And the fourth one is ferromagnetism due to the ferromagnetic clusters or secondary phases.[11, 12] Therefore, it is necessary to decide on a case-by-case basis which mechanism is applicable. In our work, we apply the first class of approach based on the mean-field theory for carrier-induced ferromagnetism in a DMS.[13, 14, 15]

Using ideas based on the dependence of  $T_c$  of DMS on the spatial distribution of magnetic ions, and envelope functions of carriers at the lowest energy subband in a confining potential[15, 16, 17], we model a hybrid double quantum well (HDQW) system shown in Fig.

1 (a). The structure of  $\text{ZnO}/\text{Zn}_{1-x}\text{Mg}_x\text{O}/\text{Zn}_{1-y}\text{Li}_y\text{O}$  has the upper p-type  $\text{ZnO}$  well with an additional  $\text{Mn}$ -doped layer at the middle of the well (or at the upper edge of the well). The p-type might be achieved by the doping of group V [18, 19] or group I [20] elements. The lower well  $\text{Zn}_{1-y}\text{Li}_y\text{O}$  is the p-type ferroelectric well with spontaneous polarization  $P$ . The inverse potential profile of a hole is shown in Fig. 1 (b), for dipole up and dipole down cases respectively. Because screening lengths at the interfaces between  $\text{ZnLiO}$  and  $\text{ZnMgO}$  are assumed to be different, the potential profile is asymmetric (different values of  $V_1$  and  $V_2$ ) in region  $W_2$ . The dimension of the structure are chosen:  $W_1 = 10 \text{ nm}$ ,  $W_2 = 10 \text{ nm}$ ,  $B = 5 \text{ nm}$ , and the capping layer is  $20 \text{ nm}$ . The confinement potential is  $V_0 = -263 \text{ meV}$  with 20% of  $\text{Mg}$  per unit cell in  $\text{ZnMgO}$  barriers. [21] Because our work is applicable in a regime of low carrier density, occupying only the lowest energy subband of a heavy hole, carrier concentrations of both wells are in the order of  $10^{11}/\text{cm}^2$  [15] and the additional band bending due to carriers is small. [22]

We previously demonstrated electric field control of ferromagnetism in  $\text{Mn}$ -doped asymmetric conventional double quantum wells (CDQW) [14], but present structure is different from CDQW because of hybridizing ferroelectricity. In this work, we can obtain additional effects from the ferroelectric well due to the reversal of spontaneous depolarizing fields. We can control the number of holes around the  $\text{Mn}$ -doped layer by reversing depolarizing fields as well as applying electric fields. The main purpose of this work is to show the possibility of using ferromagnetic/ferroelectric hybrid structures to modulate  $T_c$  by reversing polarization. We can obtain two different ferromagnetic transition temperatures in the same applied electric field in HDQW.

The Hamiltonian for this system is given by

$$H = -\frac{\hbar^2}{2m^*(z)}\frac{\partial^2}{\partial z^2} + V_c(z) - F_g z + V_d(z) \quad (1)$$

Throughout this calculation, we adopt atomic units  $R = m_0 e^4 / 2 \hbar^2$  for the energy unit, and  $a_B = \hbar^2 / m_0 e^2$  for the length unit, where  $m_0$  is the free electron mass. Here  $m^* = m$  and  $m$  is the hole effective mass and  $F_g$  is the carrier charge times for the applied electric fields.  $V_d$  is the potential due to the spontaneous depolarizing field. Because we would like to provide a qualitative estimation without complication, we ignore the Hartree and exchange-correlation interactions among carriers, and self-consistent solving of electrostatic potential with the Poisson equation even though the Hartree and exchange-correlation interactions

are related to the effective mass[22] and distribution of carrier spins.[23] The thickness of the barrier is enough so that we can ignore coupling by tunneling between the wells. We attempt to solve the eigenvalue problem,  $H(z) = E(z)$ , and it becomes

$$\frac{1}{m_0} \frac{d^2}{dz^2} \psi(z) - [V_c(z) - F_g z + V_d(z) - E] \psi(z) = 0: \quad (2)$$

The carrier confinement potential  $V_c(z)$  is  $V_0$  inside the wells and 0 outside the wells. The potential due to dipoles is  $V_d(z) = F_d(z - B/2) + (V_0 - V_1)$  where  $F_d$  is the spontaneous depolarizing field and  $V_1 (> 0)$  is the electrostatic potential at the interface due to screening charges[24] by the Thomas-Fermi model of screening. Signs correspond to dipole left and dipole right cases. This potential profile is shown in Fig. 1(b) with  $F_g = 0$ . We know that the general solution for Eq. (2) is a linear combination of Airy functions,  $Ai(x)$  and  $Bi(x)$ . Thus, we write

$$\psi(z) = C_1 Ai(\xi) + C_2 Bi(\xi); \quad (3)$$

where

$$\xi = (m_0 F_g + F_d)^{1/3} \left[ z - \frac{E - V_0 - V_1 + F_d \frac{B}{2}}{(F_g + F_d)} \right];$$

with  $\xi = \text{Sgn}(F_g + F_d)$  for the region  $W_2$  and

$$\xi = (m_0 F_g)^{1/3} \left[ z - \frac{V_c - E}{F_g} \right];$$

for elsewhere with  $F_g > 0$  assumed. By using boundary conditions and the continuity of wave functions and their derivatives at the boundaries of each region, we can calculate  $C_1$  and  $C_2$  and energy eigenvalues in the system numerically. In principle, we should include the effects of the exchange interaction between Mn ions and carriers on the carrier wave functions[6, 25], but we ignore these effects because our system has only a very thin Mn-doped layer. Therefore, our wave function is limited to a system with very thin Mn layers (submonolayer).[26] We write  $T_c$  in the form [13, 15]

$$T_c = \frac{S(S+1)J_{pd}^2 m}{12k_B} \frac{1}{h^2} \int dz j(z)^4 c(z): \quad (4)$$

Here,  $c(z)$  is a magnetic ion distribution function,  $J_{pd}$  is the exchange integral of carrier-spin exchange interaction, and  $S$  is a Mn ion spin. We calculate the change in the fourth power

of growth direction envelope functions,  $j(z)j^4$ , of carriers at the lowest energy subband in the HDQW as a function of the applied electric fields.

In numerical calculations, we choose physical parameters for p-type  $\text{ZnO}/\text{Zn}_{1-x}\text{Mg}_x\text{O}/\text{Zn}_{1-y}\text{Li}_y\text{O}$ , with  $x = 0.2$  and  $y = 0.05$ . The confinement potential  $V_0 = 263 \text{ meV}$ , and  $m_h^0 = 0.78$  and 1 for the well and the barrier, respectively.[21, 27] In our calculation, the exact values of  $J_{\text{pd}}$  and  $S$  are not required because we calculate the ratio of  $T_c$  in Eq. (4). Usually  $J_{\text{pd}}$  is one of the important factors in determining the size of  $T_c$ .

Figure 2 (a) shows the dependence of the ratio of ferromagnetic transition temperatures,  $T_c/T_{c0}$ , on bias voltage applied across the dipole left HDQW, for Mn center-doped (open triangle), and Mn edge-doped (closed circle) respectively. Here  $T_{c0}$  is  $T_c$  at  $F_g = 0 \text{ meV/nm}$  for the Mn center-doped CDQW without Li doping.[14] For  $\text{Zn}_{0.95}\text{Li}_{0.05}\text{O}$ , there are approximately  $1.05 \text{ dipoles/nm}^3$ , and they induce a maximum polarization of approximately  $8.77 \text{ C/cm}^2$ . While there is no depolarizing field (a full screening case) when barriers are metal, the maximum depolarizing field can be up to  $1.2 \text{ eV/nm}$  [28] when barriers are insulators (no screening charge). Our case is in between those cases, the depolarizing field  $F_d = 0.01 \text{ meV/nm}$  and the screening electrostatic potential  $V_1 = 0.02 \text{ meV}$  are used as input parameters for dipole down FES. Applied electric fields shift the envelope functions according to the change of potentials, as shown in Fig. 2 (b). Then, the effective hole concentration increases (decreases) in the Mn edge-doped layer (center-doped), and  $T_c$  increases (decreases) as a result. When  $F_g$  is less than  $2 \text{ meV}$ , there are few carriers confined at the lowest subband of the Mn doped well because of the effect of negative (dipole left)  $F_d$ .

Figure 3 shows the dependence of the ratio of ferromagnetic transition temperatures  $T_c/T_{c0}$  on bias voltage applied across the Mn center-doped HDQW for dipole down (closed circle), and dipole up (open triangle) respectively. By reversing the direction of spontaneous polarization, the change in Curie temperature occurs below  $F_g = 2 \text{ meV}$ . This effect is caused by asymmetry of electrostatic potential due to screening charges. The larger asymmetry is, the more effective the reversal is. Therefore, it is important to fabricate a sample having asymmetric potential to obtain this result. Both dipole down and dipole up cases have the same value of  $T_c/T_{c0}$  above  $F_g = 2 \text{ meV}$ , because the envelope functions of carriers depend on the potential profile of the Mn doped well (left side well), which are not affected by  $F_d$  as shown in the inset. When the coercive field of the ferroelectric well is much smaller than

the  $F_g = 2 \text{ meV}$ , the Curie temperature may change at the coercive field. But we do not take the reversal of polarization due to  $F_g$  into account, because we are interested in the regime of  $F_g$  lower than the coercive field. The inset shows the change in the potential profile due to the reversal of dipole polarization in the HDQW as a function of  $z$  at  $F_g = 4 \text{ meV/nm}$ . The potential profiles in the left-hand side well are the same regardless of the direction of dipoles. The energies of the lowest subbands are the same. These energy eigenvalues are shown in Fig. 4.

Figure 4 shows energy eigenvalues as a function of applied electric fields for HDQW. Solid lines indicate the upper energy limit of the Mn delta-doped well. The energy degeneracy occurs at  $F_g = 0$  for CDQW. When we compare the dipole right case and dipole left case of Fig. 4, the energy degeneracy at  $F_g = 0$  shifts to the left (dipole right) or to the right (dipole left), because the energy levels corresponding to the Mn doped well are the same, and only the energy levels of the FES well are shifted up (dipole right) or down (dipole left) by the depolarizing field. Therefore, the lowest subband transition occurs in the dipole left FES well case in Fig. 4(b). It causes the abrupt increase of  $T_c = T_{c0}$  in Fig. 3.

Figure 5 shows the effect of the depolarized field strength on the dependence of the ratio of ferromagnetic transition temperatures  $T_c = T_{c0}$ . We display three different depolarized field and apply the bias voltage across the Mn edge-doped and dipole left HDQW. As we expected, they have different transition points depending on the  $F_d$  values. All three lines merge into one because the potential profiles of the Mn doped well are not affected by  $F_d$ , as in Fig. 3.

In conclusion, we have proposed the DMS/FES hybrid double quantum well structure. By using the effects of the spontaneous depolarizing field from the FES well, we can modulate the ferromagnetic transition temperature of the DMS well in this system. We calculate the Curie ferromagnetic transition temperature in terms of its dependence on the envelope functions of carriers at the lowest energy subband. Through the reversal of the depolarizing field, we obtain two different ferromagnetic transition temperatures in an applied electric field. This result opens the possibility of using ferromagnetic/ferroelectric hybrid quantum structures for future multinary spin devices.

## Acknowledgments

This work was supported by Seoul City and the Korea Science and Engineering Foundation (KOSEF), through the Quantum-functional Semiconductor Research Center at Dongguk University.

- 
- [1] T. Dietl, H. Ohno, F. Matsukura, J. Cibert, and D. Ferrand, *Science* 287, 1019 (2000).
  - [2] M. Joseph, H. Tabata, and T. Kawai, *Appl. Phys. Lett.* 74, 2534 (1999).
  - [3] H. Q. Ni, Y. F. Lu, Z. Y. Liu, H. Qiu, W. J. Wang, Z. M. Ren, S. K. Chow, and Y. X. Jie, *Appl. Phys. Lett.* 79, 812 (2001).
  - [4] Q. T. Islam and B. A. Bunker, *Phys. Rev. Lett.* 59, 2701 (1987).
  - [5] T. Dietl, H. Ohno, and F. Matsukura, *Phys. Rev. B* 63, 195205 (2001).
  - [6] T. Jungwirth, W. A. Atkinson, B. H. Lee, and A. H. MacDonald, *Phys. Rev. B* 59, 9818 (1999).
  - [7] H. Akai, *Phys. Rev. Lett.* 81, 3002 (1998).
  - [8] K. Sato, H. Katayama-Yoshida, *Semicond. Sci. Technol.* 17, 367 (2002).
  - [9] M. Berciu and R. N. Bhatt, *Phys. Rev. Lett.* 87, 107203 (2001).
  - [10] A. Kaminski and S. DasSarma, *Phys. Rev. Lett.* 88, 247202 (2002); S. DasSarma, E. H. Hwang, and A. Kaminski, *Solid State Commun.* 127, 99 (2003).
  - [11] M. van Schilfgaarde and O. N. Mryasov, *Phys. Rev. B* 63, 233205 (2001).
  - [12] B. K. Rao, P. Jena, *Phys. Rev. Lett.* 89, 185504 (2002).
  - [13] T. Dietl, A. Haury, and Y. M. d'Aubigne, *Phys. Rev. B* 55, R3347 (1997).
  - [14] N. Kim, S. J. Lee, T. W. Kang, and H. Kim, *Phys. Rev. B* 69, 115308 (2004).
  - [15] B. Lee, T. Jungwirth, and A. H. MacDonald, *Phys. Rev. B* 61, 15606 (2000).
  - [16] H. Boukari, P. Kossacki, M. Bertolini, D. Ferrand, J. Cibert, S. Tatarenko, A. Wasieleski, J. A. Gaj, and T. Dietl, *Phys. Rev. Lett.* 88, 207204 (2002).
  - [17] L. Brety and F. Guinea, *Phys. Rev. Lett.* 85, 2384 (2000).
  - [18] Yanfa Yan, S. B. Zhang, and S. T. Pantelides, *Phys. Rev. Lett.* 86, 5723 (2001).
  - [19] L. G. Wang and Alex Zunger, *Phys. Rev. Lett.* 90, 256401 (2003).
  - [20] Eun-Cheol Lee and K. J. Chang, *Phys. Rev. B* 70, 115210 (2004).

- [21] A. Ohtomo, M. Kawasaki, T. Koida, K. Masubuchi, H. Koinuma, Y. Sakurai, Y. Yoshida, T. Yasuda, and Y. Segawa Appl. Phys. Lett. 72, 2466 (1998).
- [22] D. A. Broido and L. J. Sham, Phys. Rev. B 31, 888 (1985).
- [23] J. Fernandez-Rossier and L. J. Sham, Phys. Rev. B 66, 073312 (2002).
- [24] M. Y. Zhuravlev, R. F. Sabirianov, S. S. Jaswal, and E. Y. Tsymlal, Phys. Rev. Lett. 94, 246802 (2005).
- [25] M. A. Boselli, I. C. da Cunha Lima, and A. Ghazali, Phys. Rev. B 68, 085319 (2003).
- [26] J. Fernandez-Rossier and L. J. Sham, Phys. Rev. B 64, 235323 (2001).
- [27] Giuliano Coli, and K. K. Bajaj, Appl. Phys. Lett. 78, 2861 (2001); Hiroshi Tanaka and Shigeo Fujita, and Shizuo Fujita, ibid. 86, 192911 (2005).
- [28] Ref. [2] says that the spontaneous polarization and the coercive field ( $E_c$ ) are reported as 0.044 C/cm<sup>2</sup> and 2 kV/cm in bulk (Zn<sub>0.83</sub>Li<sub>0.17</sub>)O. Here we use the possible values by theoretical calculation.

FIG . 1: (a) Schematic diagram of DMS/FES hybrid double quantum wells. The upper well has a 0.5 monolayer of Mn-doped layer at the middle of the well (or at the upper edge of the well). The lower well is Li-doped ZnO with spontaneous electric polarization. (b) The potential profile of the HDQW structures (dotted line) for a dipole up (left) and dipole down (right) cases is shown. The confinement potential is  $V_0 = 263$  meV with 20% of Mg per unit cell in ZnMgO barriers.  $V_1$  and  $V_2$  are electrostatic potential due to screening charges at the interfaces.

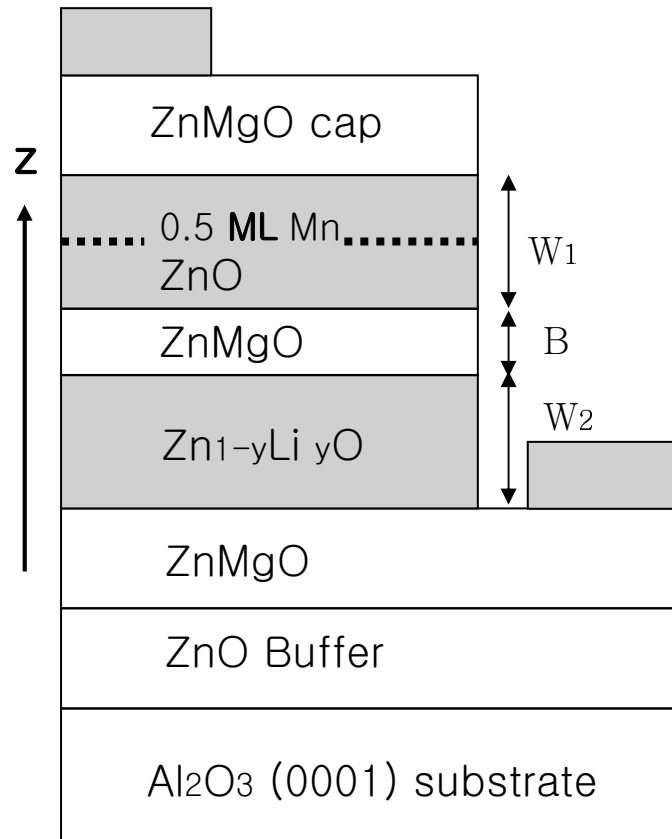
FIG . 2: (a) Dependence of the ratio of ferromagnetic transition temperatures  $T_c/T_{c0}$  on bias voltage applied across the dipole left HDQW for Mn center-doped (open triangle) and Mn edge-doped (closed circle) respectively. The system size is  $W_1 = 10$  nm,  $W_2 = 10$  nm,  $B = 5$  nm. Here  $T_{c0}$  is  $T_c$  at  $F_g = 0$  meV/nm for the Mn center-doped conventional DQW without Li doping. (b) Change in the fourth power of the growth direction envelope functions of carriers at the lowest energy subband (upper panel), and the potential profile (lower panel) in the HDQW as a function of  $z$  at  $F_g = 3$  meV/nm (solid) and  $7$  meV/nm (dashed).

FIG . 3: Dependence of the ratio of ferromagnetic transition temperatures  $T_c/T_{c0}$  on bias voltage applied across the Mn center-doped HDQW for dipole left (closed circle) and dipole right (open triangle) respectively. Inset shows the change of the potential profile due to the reversal of dipole polarization in the HDQW as a function of  $z$  at  $F_g = 4$  meV/nm.

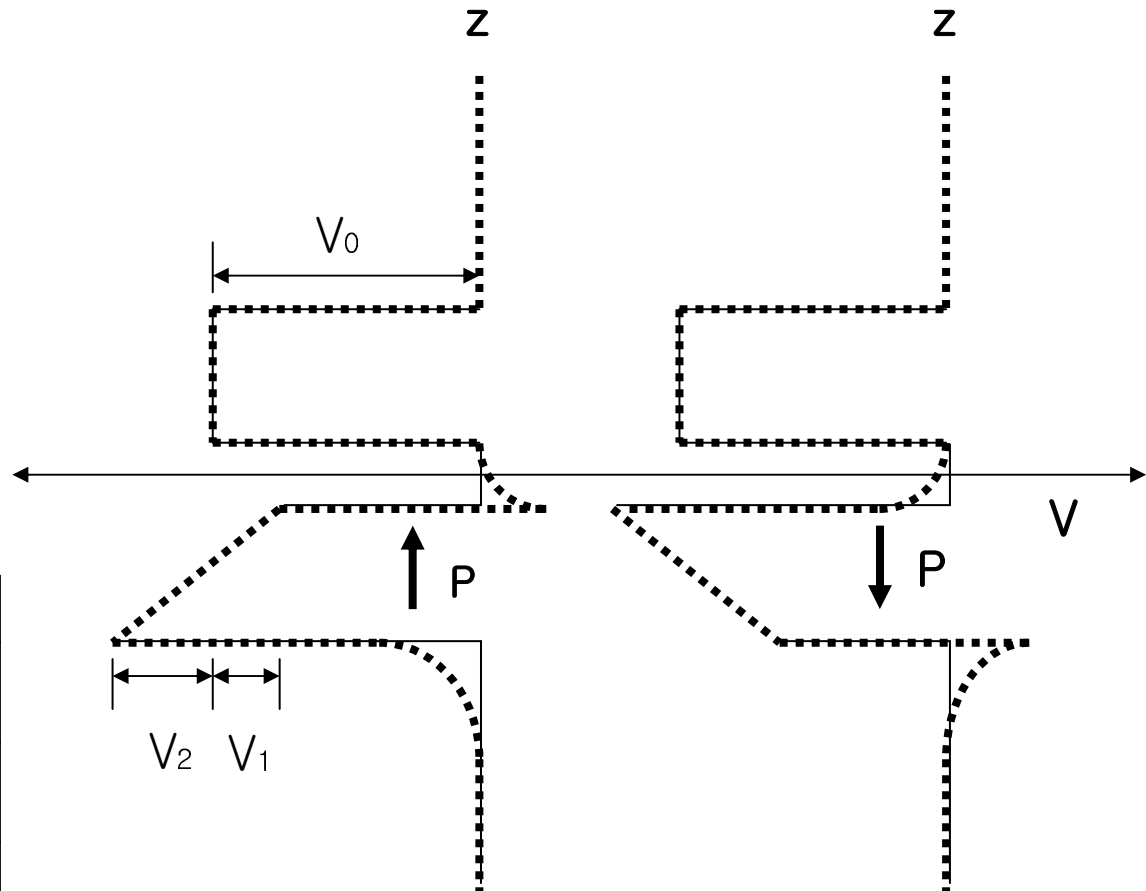
FIG . 4: Energy eigenvalues as a function of applied electric fields for hybrid double quantum wells for (a) dipole right and (b) dipole left cases. Solid lines indicate the energy upper limit of Mn delta-doped well.

FIG . 5: Dependence of the ratio of ferromagnetic transition temperatures  $T_c/T_{c0}$  on bias voltage applied across the Mn edge-doped and dipole left HDQW for different depolarized electric fields.

(a)

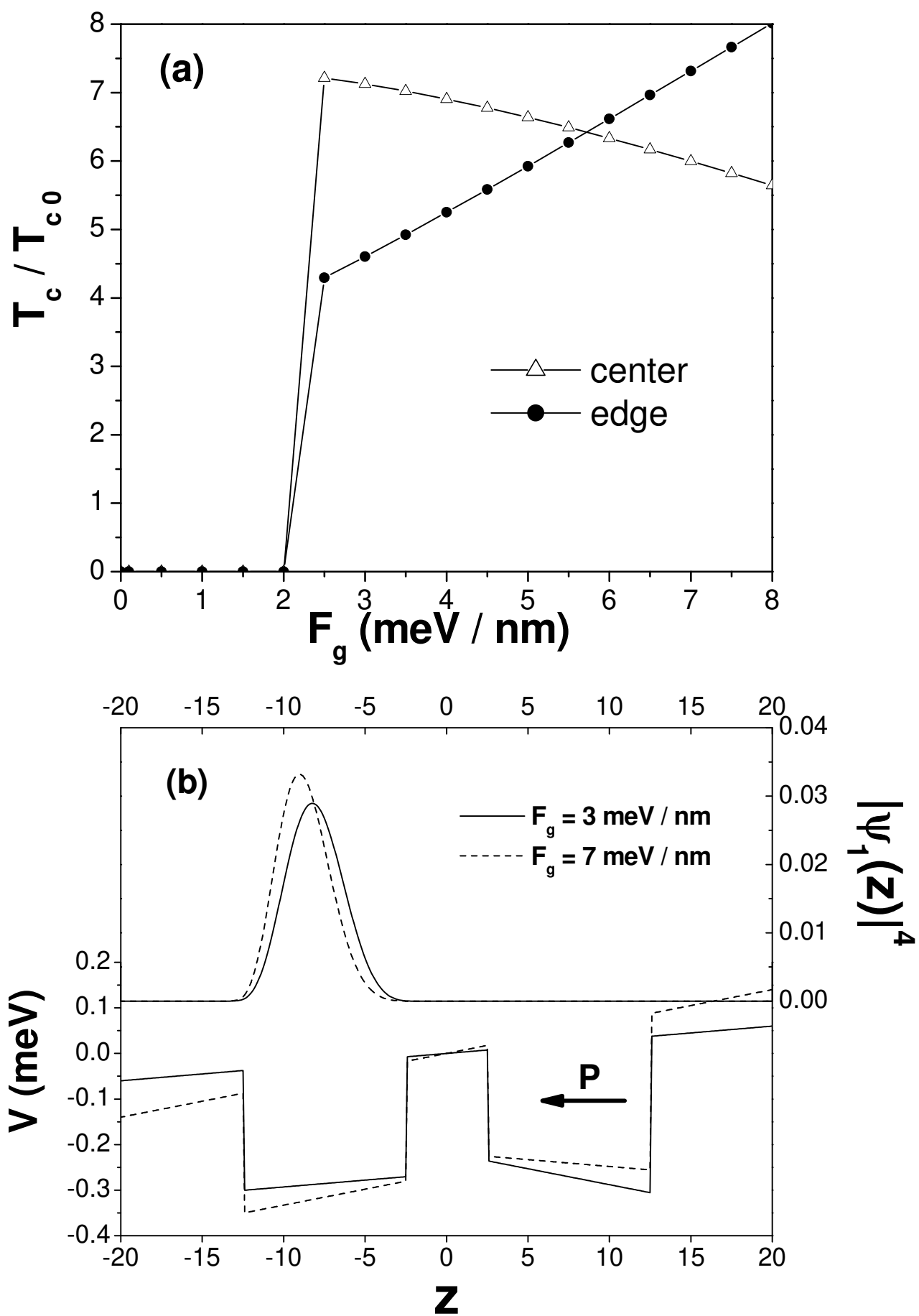


(b)



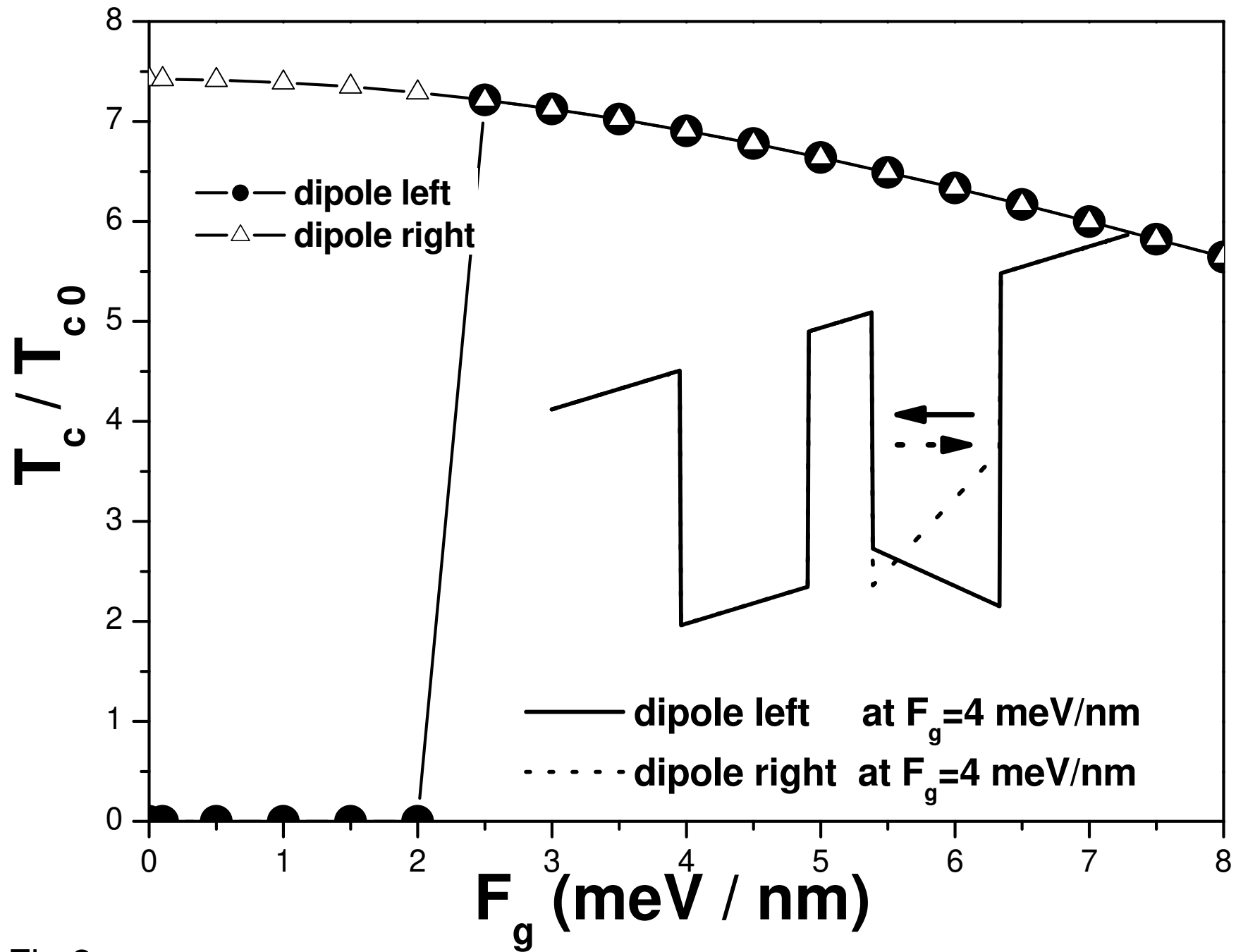
Kim-Fig. 1





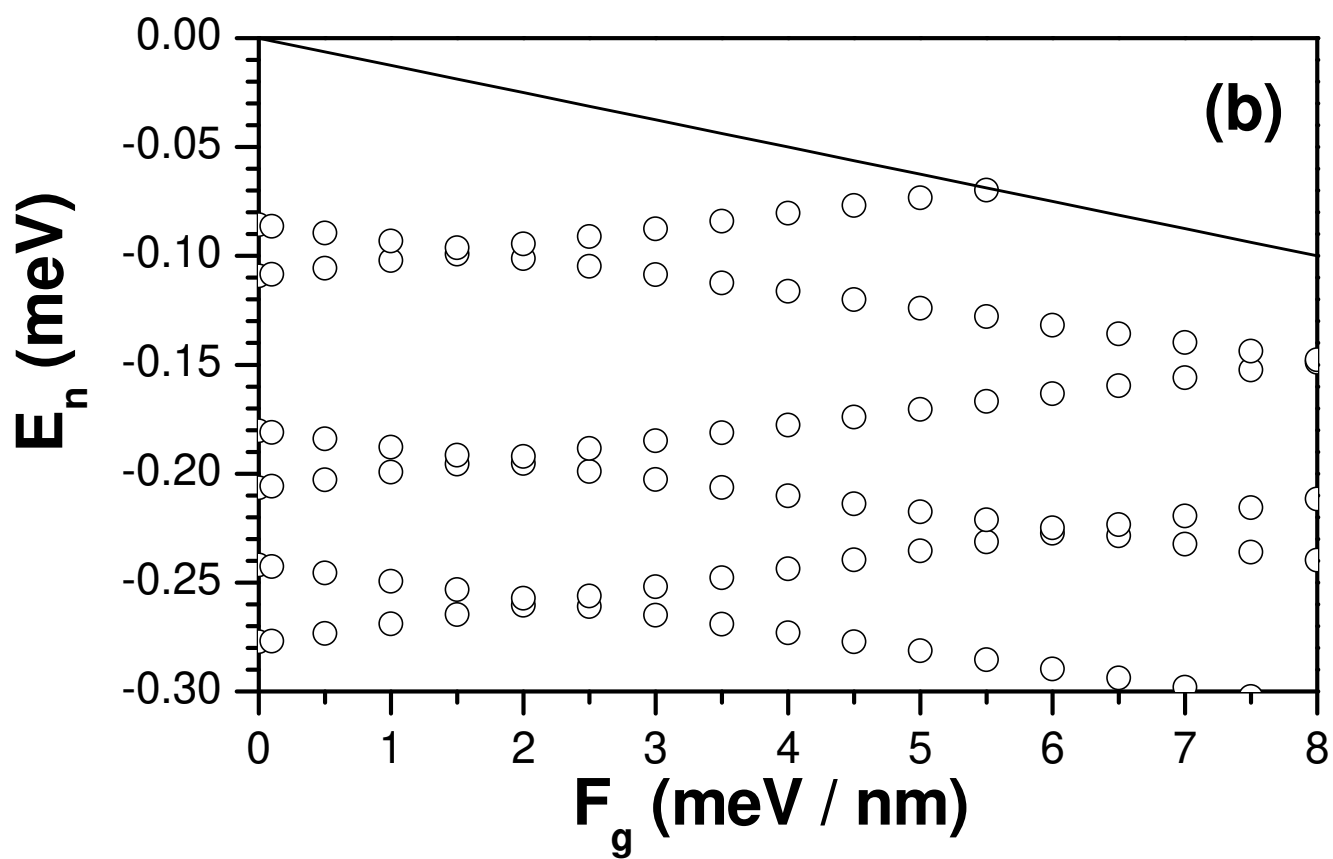
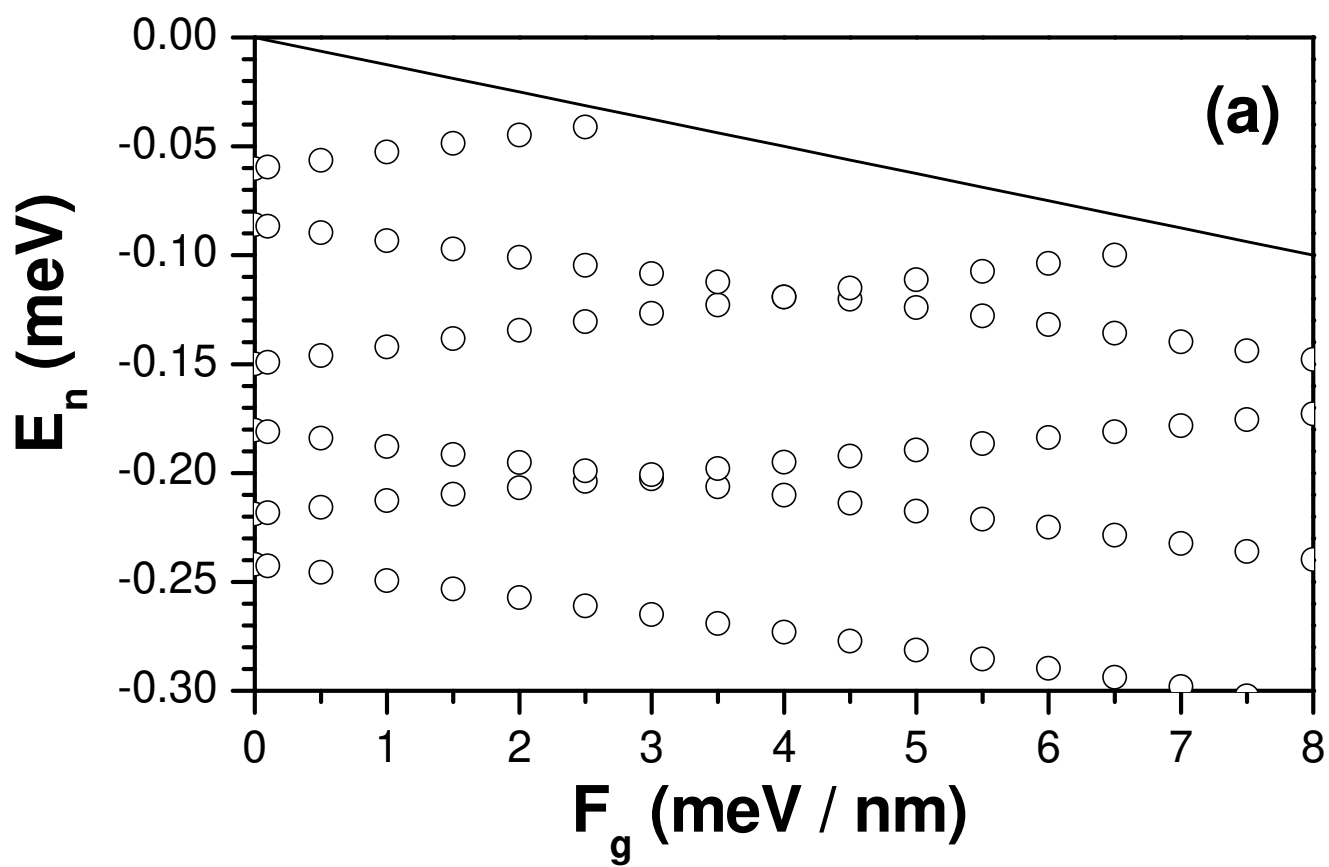
Kim-Fig. 2



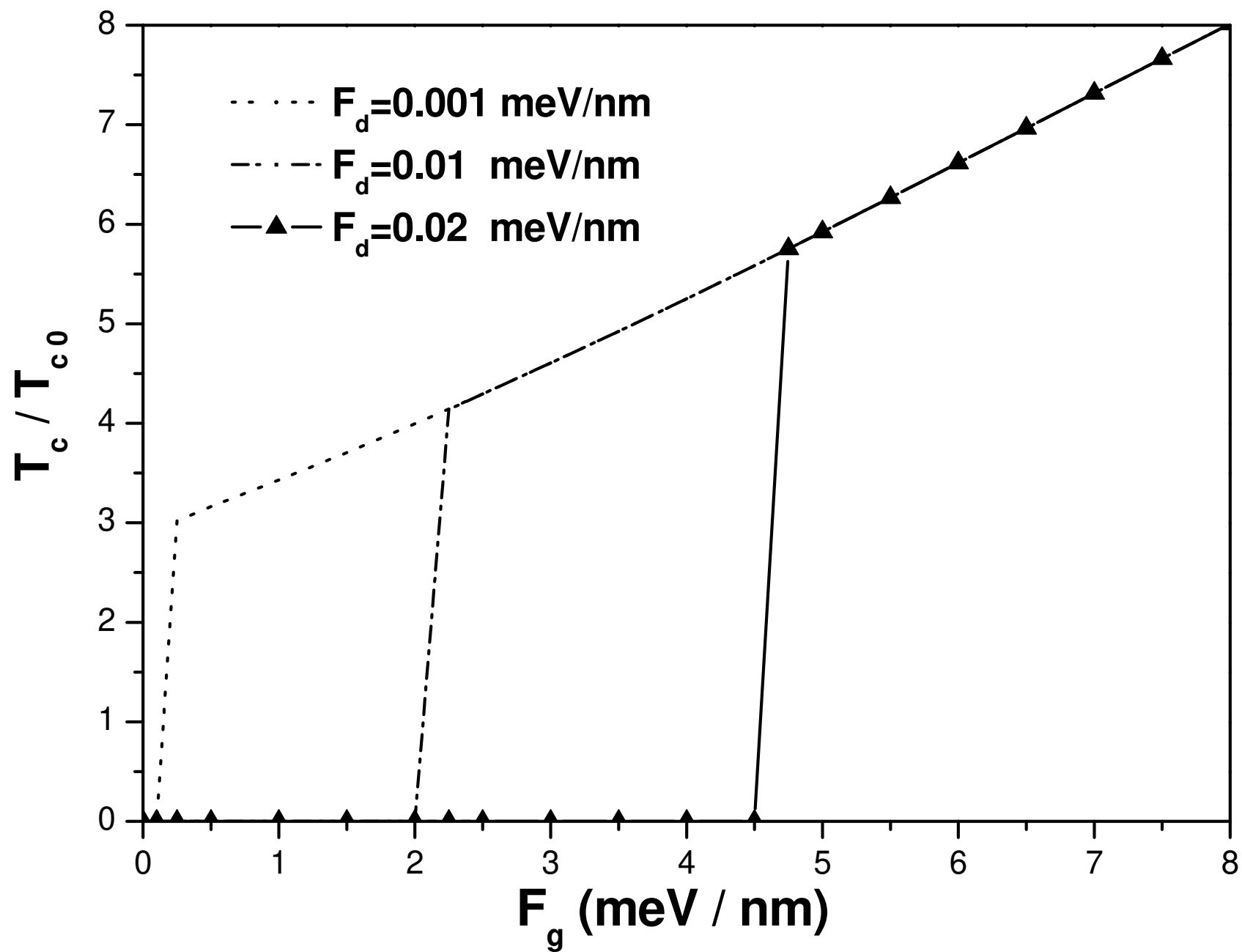


Kim-Fig.3









Kim-Fig. 5

